THE JOURNAL OF PHYSICAL CHEMISTRY B

pubs.acs.org/JPCB Article

Electric Field Effect on Condensed-Phase Molecular Systems. X. Interconversion Dynamics and Vibrational Stark Effect of Hydrogen Chloride Clusters in an Argon Matrix

Hani Kang, Youngwook Park, Sunghwan Shin, and Heon Kang*

Cite This: J. Phys. Chem. B 2020, 124, 4581−4589 Read Online

ACCESS | Metrics & More | Article Recommendations | Supporting Information

ABSTRACT: In this study, the effect of a strong ($\lesssim 4 \times 10^8$ V·m^{-1}) dc electric field on hydrogen chloride (HCl) dimers and trimers isolated in a solid argon matrix has been investigated using the ice film nanocapacitor and reflection−absorption infrared spectroscopy methods. The H−Cl vibrational bands of the HCl dimers showed a linear Stark frequency shift and an increased intensity under the applied electric field, and these changes were reversible with the electric field strength. This behavior indicated that the dimers were reoriented by the applied electric field. The reorientation occurred via tunneling inversion of individual HCl subunits of the dimer, which interconverted the proton-accepting and -donating HCl subunits, as observed for the heterodimers HCl−DCl and DCl−HCl. The interconversion of dimers could occur even at low electric field strength ($\sim 10^7$ V·m^{-1}) and was almost complete above the field strength of 1.0×10^8 V·m^{-1}. In contrast, the asymmetric H−Cl stretching bands of the HCl trimers exhibited Stark broadening under the influence of the electric field without a shift in frequency or change in intensity. This behavior indicated that the cyclic structure of the HCl trimer was stable even when subjected to a strong electric field. The Stark sensitivity factor ($\Delta\mu$) of H−Cl vibrations was deduced from the Stark effect analysis of the HCl dimer and trimer bands, which gave the following: $\Delta\mu_{D1} = 2.3 \pm 0.2$ cm^{-1}/(10^8 V·m^{-1}) for the proton-acceptor subunit of the dimer, $\Delta\mu_{D2} = 5.1 \pm 0.5$ cm^{-1}/(10^8 V·m^{-1}) for the proton-donor subunit of the dimer, and $\Delta\mu_T = 4.5 \pm 0.5$ cm^{-1}/(10^8 V·m^{-1}) for the asymmetric stretching vibration of the cyclic trimer.

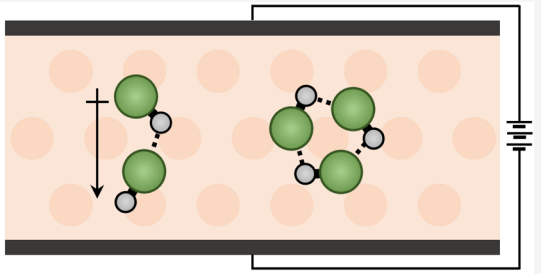

1. INTRODUCTION

In our previous study on the effect of external electric fields on hydrogen chloride (HCl) monomers isolated in a solid argon matrix,[1] we found that freely rotating HCl monomers inside the Ar matrix are pendularized by an applied dc electric field and eventually dipole-oriented along the direction of the electric field at field strengths greater than 1×10^8 V·m^{-1}. In this study, we examined the behaviors of HCl dimers and trimers isolated in the Ar matrix under the influence of a strong electric field. The effects of external electric fields with strength on the order of 10^8 V·m^{-1} on hydrogen-bonded molecular complexes are of important concern in physical chemistry because these electric field strengths correspond to those of nonspecific (mono-, di-, and quadrupole) intermolecular interactions in condensed-phase molecular environments. A systematic study of the effects of external electric fields with controlled strength on the isolated HCl clusters can provide insight into the behaviors of analogous hydrogen-bonded molecular clusters in strong electric field environments of the condensed phases.

The structure of the HCl dimer has been studied previously in the matrix-isolated environment,[2−6] superfluid helium droplets,[7] and gas phase.[8−11] In the gas phase, the HCl dimer has a nearly orthogonal, open-chain structure,[8,10] in which the angle between two hydrogen-bonded monomer units is almost 90°. The intramolecular hydrogen-bond energy of the HCl dimer was estimated to be 5.16 ± 0.26 kJ·mol^{-1}.[9] Electrostatic hexapole field experiments[11] revealed that the dipole moment of the HCl dimer is 1.5 D. Inside the Ar matrix, the HCl dimer has an open-chain structure as well.[2] Although some earlier studies have proposed a cyclic structure of the HCl dimer in the Ar matrix,[3,6] reinterpretation of experimental results and additional evidence indicate an open-chain structure.[2,5] The HCl trimer is known to have a cyclic structure both in the gas phase[12−15] and in an Ar matrix,[2,6] according to high-resolution infrared spectroscopy. Therefore, an isotopically pure HCl trimer has zero permanent dipole moment. Unlike the HCl monomer, the HCl dimer and trimer cannot rotate inside the Ar matrix. Theoretical calculations indicate that larger HCl clusters, from trimer to hexamer, have cyclic global-minimum structures.[14]

Received: March 26, 2020
Revised: May 8, 2020
Published: May 15, 2020

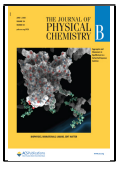

https://dx.doi.org/10.1021/acs.jpcb.0c02652
J. Phys. Chem. B 2020, 124, 4581−4589

In the gas phase, the HCl dimer and hydrogen fluoride (HF) dimer undergo interconversion tunneling dynamics.[8,10,11,16] Extremely rapid tunneling occurs between two equivalent forms of the HCl dimer comprising orthogonally oriented monomer units, which corresponds to resonant tunneling in a symmetric double-well potential.[7,9,10] The interconversion tunneling of the HF dimer is relatively slower.[15] The interconversion dynamics of gaseous HF and HCl dimers can be quenched by an external electric field.[11,16] It has been shown that the tunneling in HF dimers is quenched by applying a dc electric field with strength of up to 1.5×10^7 V·m^{-1} to a molecular beam at a low rotational temperature.[16] Also, the tunneling in HCl dimers is quenched by an electrostatic hexapole field.[11] In contrast, according to spectroscopic observations, the HCl dimer inside the cavity of an Ar matrix does not undergo interconversion tunneling.[2] In this study, we show that an external dc electric field compels HCl dimers to undergo tunneling interconversion inside the Ar matrix by means of an electrostatic brute force.

2. EXPERIMENTAL METHODS

The experiments were carried out in an ultrahigh-vacuum (UHV) chamber,[1] which was equipped with a low-energy Cs^+ ion gun, Kelvin work-function probe, Fourier transform infrared (FTIR) spectrometer, and quadrupole mass spectrometer (QMS). The samples were prepared on a Pt(111) substrate cooled to 10 K by a closed cycle He refrigerator. A thin film sample containing HCl monomers and clusters isolated in a solid Ar matrix (referred to as "HCl@Ar") was prepared by coadsorption of HCl and Ar gases in a predetermined pressure ratio. The sample had a stacked structure of an HCl@Ar film sandwiched between two Ar spacer layers. The spacer layers protected the matrix-isolated species from interfacial effects. The upper Ar layer was capped by an amorphous H_2O film to make an ice film nanocapacitor. A dosing tube was used to guide HCl gas close to the Pt(111) surface with minimal contamination of the chamber wall. Ar and H_2O gases were introduced by backfilling the chamber. Ar (99.999%) and HCl (Sigma-Aldrich, >99%) gases were used as received in commercial gas cylinders. Deionized water was purified by freeze–pump–thaw cycles before use. DCl in aqueous solution (35 wt % in D_2O, 99 atom % D in solution) was used as a source of DCl vapor, based on the fact that the vapor pressure of DCl is higher than that of water at room temperature.[17] The DCl aqueous solution was purified by freeze–pump–thaw cycles.

The thicknesses of the constituent films and the amount of condensed gases in the sample were estimated from temperature-programmed desorption (TPD) measurements.[1] The thickness of the H_2O film was estimated by comparing its TPD peak area with that of an H_2O monolayer on Pt(111). The thickness of the Ar film was determined by comparing its TPD peak area with that of the H_2O film, taking into account the different ionization cross sections of the gases in mass spectrometric detection.[18,19] One monolayer (ML) of amorphous solid water and solid Ar corresponds to a thickness of 5.5 and 5.7 Å, respectively, according to the densities of these molecular films at 10 K.[20−22]

A dc electric field was applied across the sample using the ice film nanocapacitor method.[23] A low-energy alkali-metal ion gun (Kimball Physics) was used to uniformly deposit Cs^+ ions on the surface of the H_2O capping layer of the ice film nanocapacitor. The voltage developed across the ice film nanocapacitor was measured by a Kelvin work-function probe. To decrease the voltage, low-energy electrons were sprayed on the H_2O film surface using the QMS filament. The field strength applied across the HCl@Ar film in the ice film nanocapacitor structure was estimated using eq 1.

$$F = \frac{V}{d_{Ar} + d_{H_2O}\frac{\varepsilon_{Ar}}{\varepsilon_{H_2O}}} \quad (1)$$

where V is the voltage across the ice film capacitor as measured by a Kelvin probe, d_{Ar} and d_{H_2O} are thicknesses of the corresponding films, and ε_{Ar} and ε_{H_2O} are the relative permittivities with values of 1.6 and 2,[24,25] respectively.

Reflection–absorption infrared spectroscopy (RAIRS) measurements were performed at a grazing angle of 85° using a FTIR spectrometer equipped with a mercury–cadmium-telluride detector. The IR beam was p-polarized using a wire grid polarizer placed in the incident beam path. The RAIR spectra were scanned 2304 times at a spectral resolution of 1 cm^{-1}.

3. RESULTS AND DISCUSSION

3.1. RAIR Spectra of HCl Dimers and Trimers in an Ar Matrix. We performed RAIRS measurements for the HCl@Ar sample, which was prepared in the ice film nanocapacitor structure, as shown in Figure 1c. Figure 1a shows the RAIR spectra of the HCl monomers, dimers, and trimers in the sample at various strengths of the applied electric field. The vertical arrows on the abscissa of Figure 1a designate the position of peaks that are observed or expected to appear in the zero-field spectrum.[2,4,6] They are R(0) ($[\nu = 0, J = 0] \rightarrow [\nu = 1, J = 1]$, 2888 cm^{-1}), Q ($[\nu = 0, J = 0] \rightarrow [\nu = 1, J = 0]$, 2871 cm^{-1}), and P(1) ($[\nu = 0, J = 1] \rightarrow [\nu = 1, J = 0]$, 2853.5 cm^{-1}) transitions of the HCl monomer, D1 (2855.5 cm^{-1}), and D2 (2818 cm^{-1}) peaks of the HCl dimer, which are H–Cl stretching vibrations of the proton-accepting (or free) and proton-donating (or bound) HCl subunits of the dimer, respectively, and T (2787 cm^{-1}) peak corresponding to the asymmetric stretching vibration of the HCl trimer. The quoted frequencies are for the major isotope ($H^{35}Cl$) species. The vibrations of the $H^{37}Cl$ monomer and dimer appear as weak shoulders of the major isotope peaks at frequencies lower by ~2 cm^{-1}. The structures of the HCl dimer and trimer are sketched in Figure 1b based on information from previous studies.[2,8,10]

The spectral position and shape of these peaks changed as the strength of the applied electric field was increased. The change in peak positions has been traced by black dotted lines (Figure 1a). For the HCl monomer, the R(0) peak disappeared and the Q peak appeared as the electric field strength was increased. The changes in the R(0) and Q bands of the monomer have been discussed in a previous study in terms of pendularization and alignment of HCl monomers under the electric field.[1] The D1 and D2 peaks of the HCl dimer increased in intensity and were red-shifted in frequency. The two peaks showed very different field sensitivities in these behaviors. The T peak of the HCl trimer became broadened and split into two components at high field strength. All these changes occurred reversibly with respect to an increase or decrease in the field strength. In the present study, we have only focused on the spectral features of the HCl dimer and trimer.

https://dx.doi.org/10.1021/acs.jpcb.0c02652
J. Phys. Chem. B 2020, 124, 4581−4589

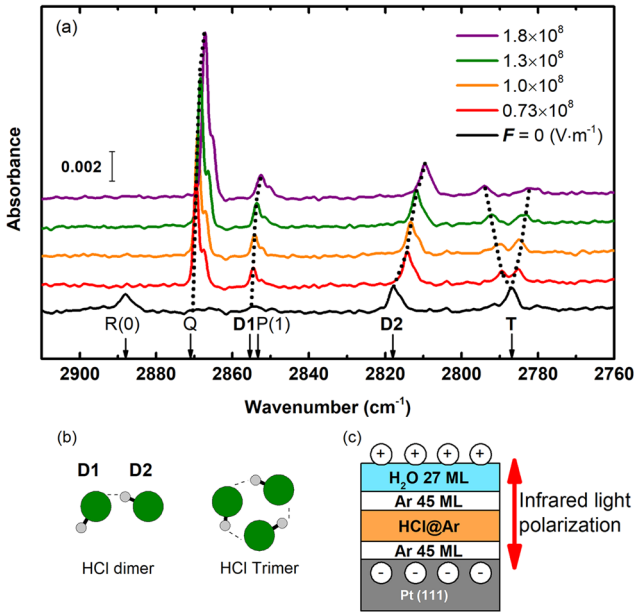

Figure 1. (a) RAIR spectra of HCl monomers, dimers, and trimers isolated in an Ar matrix at 10 K, measured as a function of the strength of the applied electric field. The spectra are displayed in the order of increasing field strength from the bottom (zero field; black trace) to the top (1.8×10^8 V·m^{-1}; violet trace). The temporal sequence of spectral acquisition in the experiment was black → orange → purple during the increase of the field and then green → red during the decrease of the field. The continuous changes in spectral features observed during the increase and decrease in field strength demonstrate the reversibility of the field-induced spectral changes. The changing peak positions are guided by the black dotted lines. The arrows at the bottom abscissa indicate major peak positions in the zero-field spectrum (see text). (b) An open-chain structure of HCl dimer and a cyclic structure of HCl trimer. The small gray balls are hydrogen atoms, and the large green balls are chlorine atoms. (c) A schematic drawing of the ice film nanocapacitor structure containing an HCl@Ar film. The direction of light polarization (red arrow) was parallel to the direction of the applied electric field. The Ar:HCl molar ratio in the HCl@Ar film was 340:1.

Effect of Electric Field on Vibrational Frequencies. It is known that the HCl dimer in an Ar matrix has an open-chain structure consisting of the proton-donating (D2) and proton-accepting (D1) HCl subunits (Figure 1b).[2] The applied electric field shifted the D1 and D2 bands to a lower frequency, and the shift of the former occurred to a lesser degree. Figure 2 shows the plots of the peak positions of the D1 and D2 bands of the HCl dimer against the electric field strength. The plot for the Q band of the HCl monomer is also shown for comparison.[1] The plots show a linear proportionality between the frequency shift and electric field strength over the range of $(1-4) \times 10^8$ V·m^{-1}, with a slight change in the slope in the lower field region ($<1 \times 10^8$ V·m^{-1}). The red-shift in the peak position and its reversible behavior with the change in field strength suggest its origin as the vibrational Stark effect (VSE) of H−Cl oscillators that are oriented along the field direction.[1] The vibrational frequency shift ($\Delta\tilde{\nu}$) of an individual oscillator owing to the Stark effect in an electric field ($\vec{F}$) is expressed by eq 2.[26]

$$\Delta\tilde{\nu} = -\frac{1}{hc}(\Delta\vec{\mu}\cdot\vec{F} + \cdots) \quad (2)$$

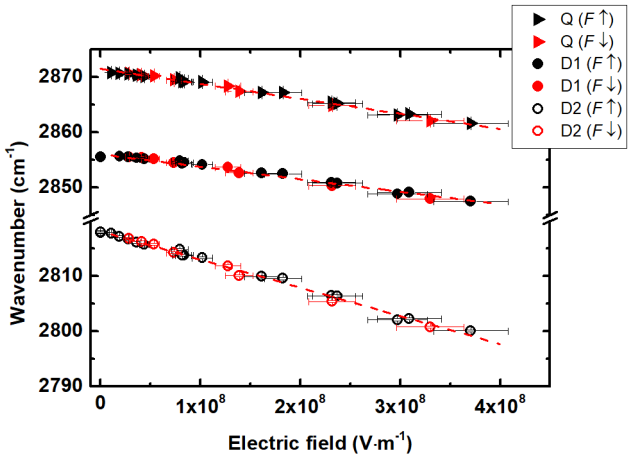

Figure 2. Frequency shifts of Q, D1, and D2 bands versus the strength of the applied electric field. Data points obtained from six different samples with different Ar:HCl molar ratios, (190−400):1, are shown overlapped in this plot. Black points are the frequency shifts measured during the increase in field strength, and red ones are during the decrease in field strength. Red dashed lines are linear fits to data points.

where $\Delta\vec{\mu}$ is the vibrational Stark sensitivity factor or the Stark tuning rate.

According to eq 2, the red-shift in frequency indicates that the sign of $\Delta\vec{\mu}\cdot\vec{F}$ is positive and the molecular dipole of HCl is oriented along the direction of the applied field ($\vec{\mu}\cdot\vec{F} > 0$) because the permanent dipole ($\vec{\mu}$) and difference dipole ($\Delta\vec{\mu}$) vectors are parallel for HCl. However, it is known that HCl dimers are randomly oriented in the Ar matrix, and the D1 and D2 subunits of the dimers can also be expected to be so in the absence of an external electric field. Oscillators with an isotropic orientational distribution cannot produce a unidirectional Stark frequency shift.[26] Therefore, this observation indicates that each subunit is dipole-oriented along the direction of the electric field. The linear proportionality between the frequency shift and field strength above $\sim 1 \times 10^8$ V·m^{-1} indicates that the dipole orientation occurs to near completion above this field strength. Note that in the present experiment using a polarized light, the dimers with their Cl−Cl axis parallel to the field direction were preferentially detected, while those with Cl−Cl axis perpendicular to the field direction did not contribute to the spectral absorbance significantly. Accordingly, the observed Stark behaviors originated largely from the former species. A detailed discussion of the field-induced dipole orientation is given in Section 3.2.

The slopes of the linear fits to data points in Figure 2 give the Stark sensitivity factor (eq 2) of the vibrations. The estimated values of $|\Delta\vec{\mu}|$ were the following: $\Delta\mu_Q = 2.7 \pm 0.3$ cm^{-1}/(10^8 V·m^{-1}), $\Delta\mu_{D1} = 2.3 \pm 0.2$ cm^{-1}/(10^8 V·m^{-1}), and $\Delta\mu_{D2} = 5.1 \pm 0.5$ cm^{-1}/(10^8 V·m^{-1}). It is noteworthy that $\Delta\mu_Q$ and $\Delta\mu_{D1}$ are close to each other, whereas $\Delta\mu_{D2}$ is about twice as large as the former sensitivity factors. The difference is attributed to the fact that the proton in D2 is hydrogen-bonded to its neighbor, whereas the protons of Q and D1 are not. For accurate comparison of the Stark sensitivities, it should be noted that the local field correction will be necessary. The actual field strength (F_{local}) that a matrix-isolated molecule experiences is related to the external field strength (F_{ext}) by $F_{local} = c_{local}F_{ext}$, where c_{local} is the local field correction factor. Accordingly, the actual Stark sensitivity is

https://dx.doi.org/10.1021/acs.jpcb.0c02652
J. Phys. Chem. B 2020, 124, 4581−4589

expressed by $\Delta\mu_{local} = \Delta\mu/c_{local}$.[27,28] The value of c_{local} is estimated to lie between 1 and 2.[28,29] Different values of c_{local} may apply to the HCl monomer and dimer in the Ar matrix, and this may introduce a certain ambiguity in comparing these $\Delta\mu$ values. Only the uncorrected $\Delta\mu$ values are reported in this article for convenience.

We conducted similar measurements for DCl monomers and clusters isolated in the Ar matrix, and the results are shown in Figure S1 in the Supporting Information. The Stark sensitivities of the corresponding DCl bands were estimated to be $\Delta\mu_{Q}^{DCl} = 1.3 \pm 0.2$ cm^{-1}/(10^8 V·m^{-1}), $\Delta\mu_{D1}^{DCl} = 1.3 \pm 0.2$ cm^{-1}/(10^8 V·m^{-1}), and $\Delta\mu_{D2}^{DCl} = 3.6 \pm 0.4$ cm^{-1}/(10^8 V·m^{-1}). These $\Delta\mu$ values for the DCl bands are approximately 1.4 times smaller than those of the HCl bands, as expected from the H/D isotopic effect.

Effect of Electric Field on Absorbances. The applied electric field increased the absorbance of both D1 and D2 bands (Figure 1a). However, the relative increase in absorbance was much larger for D1 than that for D2. Figure 3 indicates the relative changes in the absorbances of D1 and D2 bands versus the electric field strength. The normalized absorbances are plotted for this purpose, which are defined as the absorbance at a certain field strength (A) divided by the absorbance at zero field (A_0). Because the zero-field absorbance of the D1 band is extremely weak, a thick reference sample of HCl@Ar was prepared (not shown) to obtain a reliable estimate of the A_0 of D1 in the spectrum with a good signal-to-noise (S/N) ratio. The intensity of the overlapping P(1) band of the HCl monomer was subtracted in this estimation. The estimated A_0 ratio of D1 to D2 was ~0.085 ± 0.020, which was used for the plots in Figure 3. Previous studies[2,30] report this ratio as having a value of 0.12 ± 0.06 from similar analyses; these two numbers are consistent within the uncertainty range.

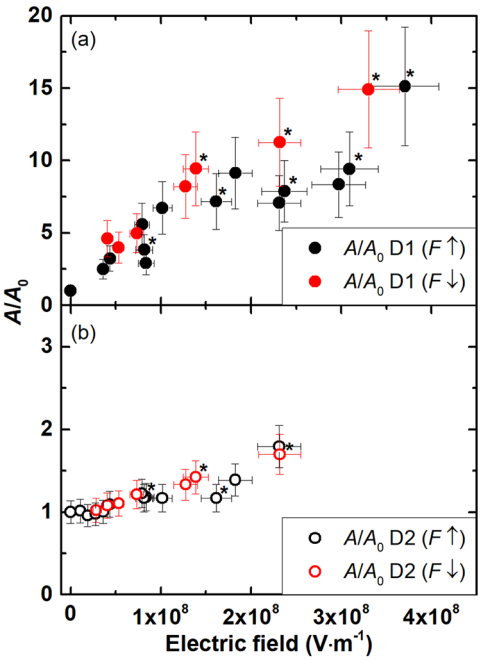

Figure 3. Plots of the normalized absorbance (A/A_0) versus the electric field strength for D1 and D2 bands, where A indicates the absorbance in the electric field, and A_0 the absorbance at zero field. Data points obtained from six different samples with varying Ar:HCl ratios of (190−400):1 are shown overlapped in one plot. (a) The A/A_0 ratio of the D1 band. The relatively large uncertainty in A/A_0 is related to the low S/N ratio of the D1 band at zero field. (b) The A/A_0 ratio for the D2 band. The data points for D2 are shown only below 2.5 × 10^8 V·m^{-1} because the D2 band overlapped with the T band above this field strength. Black-colored points were measured during the increase of the field strength, and red-colored points were measured during the decrease of the field strength. The asterisks mark the data points from samples that have a higher population of trimers than dimers.

Figure 3 shows that the absorbance of D1 increased 10 times or more as the field strength increased above 2 × 10^8 V·m^{-1}. On the other hand, the absorbance of D2 increased only slightly, less than twice at this field strength. Therefore, it became necessary to determine if these behaviors were related to the reorientation of the D1 and D2 subunits in the applied electric field. The field-induced reorientation of oscillators toward the field direction can increase absorbance because the light polarization vector is collinear with the applied electric field in the present experiment. When randomly oriented oscillators become perfectly field-aligned, A/A_0 increases asymptotically to a value of 3 according to the Langevin formula.[29] In the HCl dimer, the proton-accepting (D1) subunit was likely oriented by the applied field. The reorientation, however, could not increase the absorbance of D1 more than threefold. It was difficult to reorient the proton-donating (D2) subunit because of the strong internal hydrogen bonding (5 kJ·mol^{-1})[9] for the dimer, which was 2 orders of magnitude larger than the dipole field interaction energy and because the whole dimer structure could not be reoriented inside the matrix. Thus, it was evident that effects other than molecular reorientation also needed to be considered.

The linear, unidirectional frequency shift of the D1 band with an increase in the field strength above ~1 × 10^8 V·m^{-1} (Figure 2) indicates that the field orientation of the D1 subunit was almost complete at this field strength. Yet, the A/A_0 value of D1 continually increased at higher field strengths to a value much greater than 3. This extra increase in the absorbance could be attributed to an increase in the transition dipole moment of the D1 vibration in a strong electric field.[31] The actual field strength that D1 experienced inside the matrix was likely higher than the externally applied field strength on the order of 10^8 V·m^{-1}. Because the proton in the field-oriented D1 subunit was positioned close to the cavity wall of the dielectric matrix, the local field exerted on D1 could be significantly enhanced by the polarization of the matrix.[29,32] The relatively small (1.5 times) increase in A/A_0 of D2 may similarly be caused by the field-induced increase in the vibrational transition dipole moment. For D2, however, the local field enhancement effect was likely weaker than that for D1 because its proton charge was shielded by the neighboring Cl atom and positioned farther away from the matrix cavity wall. Accordingly, the associated increase in the transition dipole moment of the D2 vibration was probably smaller.

In the above discussion, we have excluded the possibility that larger HCl clusters dissociate to HCl dimers under the influence of the electric field and contribute to the increased absorbance of the D1 band. This interpretation is supported by the plots in Figure 3, which show that the observed change in A/A_0 with field strength was independent of the relative populations of the HCl dimer and trimer in the samples. It shows that the absorbance of D1 was mostly attributable to HCl dimers and unaffected by the population of larger HCl clusters.

https://dx.doi.org/10.1021/acs.jpcb.0c02652
J. Phys. Chem. B 2020, 124, 4581−4589

3.2. Interconversion of Dimers. The unidirectional frequency shifts of the D1 and D2 bands (Figure 2) indicate the orientation of D1 and D2 subunits along the direction of the applied field. In the absence of the reorientation of the whole dimer structure, this observation indicated that the individual subunits were dipole-inverted by the electric field. This process changed the role of the proton-donor and proton-acceptor subunits in the dimer, such that D1 became D2 and vice versa. However, the relative populations of D1 and D2 did not change, and neither did the absorbance of their bands. While the experimental observations for the $(HCl)_2$ dimer were consistent with this proposed mechanism, they did not unambiguously prove the mechanism. We further investigated the dipole-inversion mechanism for dimer interconversion by conducting experiments with (HCl)(DCl) heterodimers.

Gas-phase measurements reveal that the HCl−DCl structural isomer (i.e., a hydrogen-bond isomer with a proton-accepting HCl and proton-donating DCl) is more stable than the DCl−HCl structural isomer by 0.19 ± 0.05 kJ·mol^{-1} because of the difference in their zero-point energies.[10] Therefore, the former isomer has a higher Boltzmann population than the latter. If an external electric field interconverts the proton-acceptor (D1) and proton-donor (D2) subunits in the dimer, then it would change the relative populations of the two isomers and their relative absorbances. Figure 4 shows the D1 and D2 bands in the spectra of the samples containing HCl and DCl in different (2:1 and 1:2) molar ratios and the changes under the influence of an electric field (7.5×10^7 V·m^{-1}). For the 2:1 HCl−DCl mixture (Figure 4a), the absorbance of ν_{donor}^{HCl} (from HCl−HCl and DCl−HCl isomers) was increased by the electric field, and that of ν_{donor}^{DCl} (from HCl−DCl and DCl−DCl isomers) was slightly decreased. The results for the 1:2 mixture sample confirmed the same trend (Figure 4b). These results indicate a net population change from HCl−DCl to DCl−HCl under the electric field. As illustrated by a molecular cartoon in Figure 4c, the interconversion between HCl−DCl and DCl−HCl isomers can occur via field-induced inversion of individual HCl and DCl subunits. However, because of the higher Boltzmann population of the HCl−DCl isomer than the DCl−HCl isomer, a net population change occurs from the former to the latter.

The electric field increased the absorbances of $\nu_{acceptor}^{HCl}$ and $\nu_{acceptor}^{DCl}$ also. The large increase in oscillator strength of these bands (Figure 3a) must have a dominant effect on these phenomena. Although the population of proton-accepting HCl subunits is decreased by tunneling interconversion, this effect must be relatively minor.

Figure 5 displays the plots of the absorbances of the D2 bands, i.e., ν_{donor}^{HCl} and ν_{donor}^{DCl}, as a function of the applied field strength. The absorbances shown are the normalized values (A/A_0) against the zero-field absorbance by considering the field-induced change in D2 absorbance, shown in Figure 3 for $(HCl)_2$. Therefore, the change in A/A_0, as shown in Figure 5, is solely because of dimer interconversion. The blue circles indicate the A/A_0 of ν_{donor}^{HCl} (from HCl−HCl and DCl−HCl isomers), and the red circles indicate the A/A_0 of ν_{donor}^{DCl} (from HCl−DCl and DCl−DCl isomers). The gradual changes in the A/A_0 curves indicate that the yield of dimer interconversion increased as the field strength was increased.

To obtain quantitative data for the change in A/A_0 with electric field strength (Figure 5), we considered the enthalpy and entropy changes associated with the dimer interconversion. This thermodynamic model is explained in detail in Section 2 of the Supporting Information. A similar approach was undertaken to understand the inversion of CO in a solid crystal in an electric field.[33] In brief, the inversion of HCl monomer units by an external electric field lowers the dipole−electric field interaction energy (enthalpy). The stabilization energy (ΔU_F) in the electric field (F) includes the energy gained by the inversion of HCl as well as the energy changed by the interconversion of HCl−DCl and DCl−HCl owing to their different formation energies. Simultaneously, the configurational entropy of the system associated with the molecular orientation is decreased by the field-induced dipole inversion of HCl. The orientation of the molecular dipole projected to the vector direction of electric field, "up" (↑) or "down" (↓), is equally populated for isotropically oriented molecules at zero field. As the dipole orientation occurs along the field direction, this population balance shifts and the configurational entropy decreases (ΔS_F). Isotopical differences of molecules are not included in this entropy calculation.

The competition between energy stabilization and entropy decrease results in an equilibrium as the interconversion of dimers occurs to a certain fraction, f, at which the free energy of the system is minimized: $\partial[\Delta U_F(f) - T\Delta S_F(f)]/\partial f = 0$,

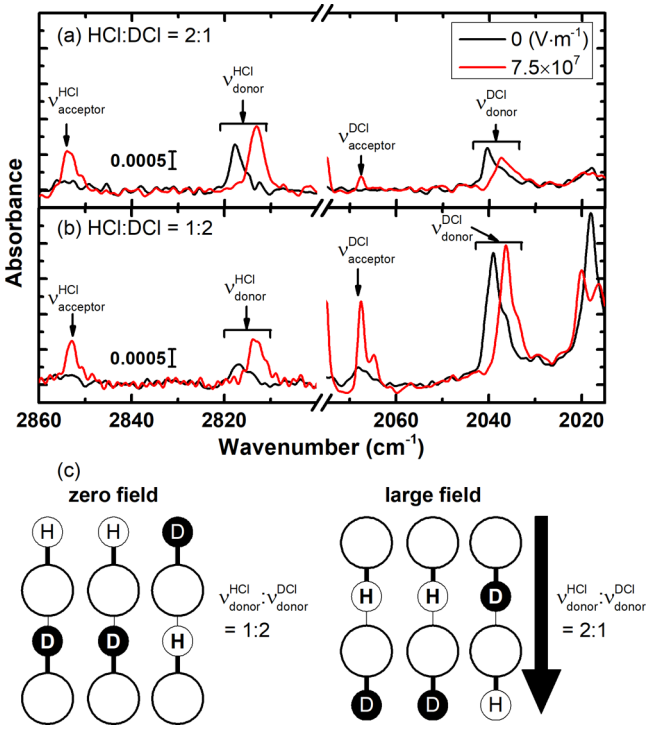

Figure 4. RAIR spectra of HCl/DCl mixture samples with different molar ratios: (a) HCl:DCl = 2:1 and (b) HCl:DCl = 1:2. The spectral intensities are contributed by HCl−DCl and DCl−HCl heterodimers as well as $(HCl)_2$ and $(DCl)_2$ homodimers in the samples. The positions of $\nu_{acceptor}^{HCl}$, ν_{donor}^{HCl}, $\nu_{acceptor}^{DCl}$, and ν_{donor}^{DCl} bands are designated by the arrows. The black traces are the zero-field spectra, and the red traces are the spectra at 7.5×10^7 V·m^{-1}. (c) A cartoon illustrating the absorbance change of ν_{donor}^{HCl} and ν_{donor}^{DCl} associated with the field-induced interconversion of HCl−DCl and DCl−HCl structural isomers. For example, a collection of HCl−DCl and DCl−HCl isomers (picture on the left side) at zero field produces the intensity ratio of ν_{donor}^{HCl}:ν_{donor}^{DCl} = 1:2. The tunneling interconversion in the electric field (the right side) changes the ratio of the isomers and the intensities to ν_{donor}^{HCl}:ν_{donor}^{DCl} = 2:1. The direction of electric field is indicated by the arrow.

https://dx.doi.org/10.1021/acs.jpcb.0c02652
J. Phys. Chem. B 2020, 124, 4581−4589

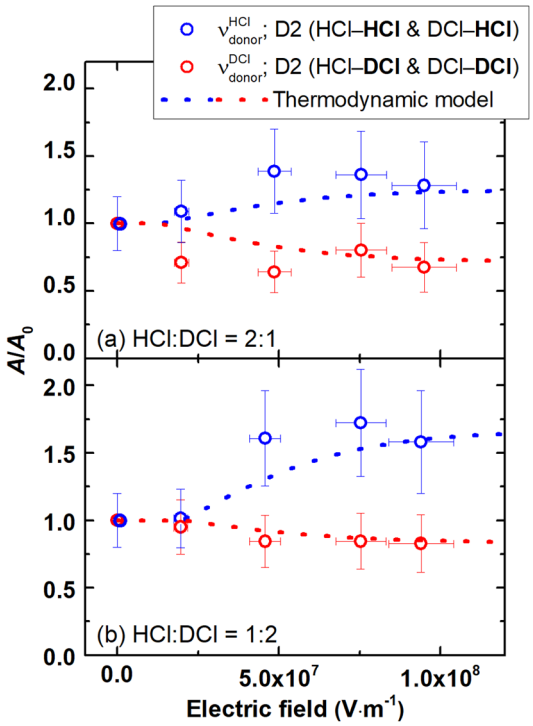

Figure 5. Plots of the normalized absorbance (A/A_0) versus the electric field strength measured for HCl/DCl mixture samples. Blue circles represent the D2 band of HCl (ν_{donor}^{HCl}) contributed from DCl–HCl and $(HCl)_2$. Red circles are the D2 band of DCl (ν_{donor}^{DCl}) from HCl–DCl and $(DCl)_2$. The dotted traces are theoretical values from a thermodynamic model (see text). (a) A HCl/DCl mixture sample with HCl:DCl molar ratio of 2:1. The blue-dotted trace increases to an asymptotic value of 1.25, and the red-dotted trace decreases to 0.7. (b) A HCl/DCl mixture sample with HCl:DCl ratio of 1:2. The blue-dotted trace approaches to 1.7, and the red-dotted trace approaches to 0.8.

where T is the temperature. The equilibrium value of f at a given field strength F is expressed by a Boltzmann distribution as shown in eq 3.

$$(0.5 + f)/(0.5 - f) = \exp[(\mu F + (1 - 2p)\Delta E)/k_B T] \quad (3)$$

where μ is the electric dipole moment (1.1 D) of HCl[34] and DCl,[35] ΔE is the energy difference between HCl–DCl and DCl–HCl isomers, p is the Boltzmann population ratio of the two structural isomers at zero field, and k_B is the Boltzmann constant. Then, by calculating the equilibrium interconversion fraction f at a given field strength from eq 3, it is possible to estimate the population ratio of HCl–DCl and DCl–HCl isomers and, in turn, A/A_0 for the corresponding D2 bands.

The A/A_0 values for ν_{donor}^{HCl} and ν_{donor}^{DCl} calculated from this model are shown by dotted lines in Figure 5. For comparison with the experimental results, which are presented on the scale of the external electric field strength without the local field correction, the theoretical electric field is divided by a local field correction factor of 1.5, as it is expected to have a value between 1.0 and 2.0.[28,29] The theoretical A/A_0 curves indicated that the dimer interconversion was already significant at the field strength of 4×10^7 V·m^{-1} and occurred almost to completion above 1×10^8 V·m^{-1}. At this field strength, ~86% of the dimers ($f = 0.36$) were oriented toward the field direction via field-induced interconversion. Complete interconversion gave A/A_0 values of 1.25 for ν_{donor}^{HCl} and 0.7 for ν_{donor}^{HCl} as shown in Figure 5a (HCl:DCl molar ratio = 2:1). In Figure 5b, the corresponding values were 1.7 for ν_{donor}^{HCl} and 0.8 for ν_{donor}^{HCl}. The thermodynamic model properly reproduces the experimental trend that the absorbance of ν_{donor}^{HCl} increases and that of ν_{donor}^{DCl} decreases as the electric field strength increases. Quantitative agreement between the experiment and the model is satisfactory, except for a few data points with substantial deviations, which confirms that the field-induced interconversion of the HCl dimer occurs by the inversion of individual HCl subunits.

For the inversion of HCl subunits to occur in the dimer, the intramolecular hydrogen bond must be broken. The zero-point dissociation energy of the dimer in the gas phase is 5.16 ± 0.26 kJ·mol^{-1}.[9] The energy barrier for the inversion of subunits is ~0.6 kJ·mol^{-1}[18] for $(HCl)_2$ in the gas phase. For comparison, the dipolar potential energy of HCl in an electric field is μF = 0.23 kJ·mol^{-1} at 1×10^8 V·m^{-1}, which is too low to overcome the energy barrier for the inversion. Therefore, it is contended that the field-induced interconversion of the dimer occurred via tunneling rather than over a classical barrier height.

3.3. Vibrational Stark Broadening of Trimers. The RAIR spectrum in the region of the HCl trimer band is shown magnified in Figure 6. In the zero-field spectrum (Figure 6a), the highest peak at 2787 cm^{-1} (T; labeled as II in Figure 6) represents the asymmetric stretching vibration of the cyclic

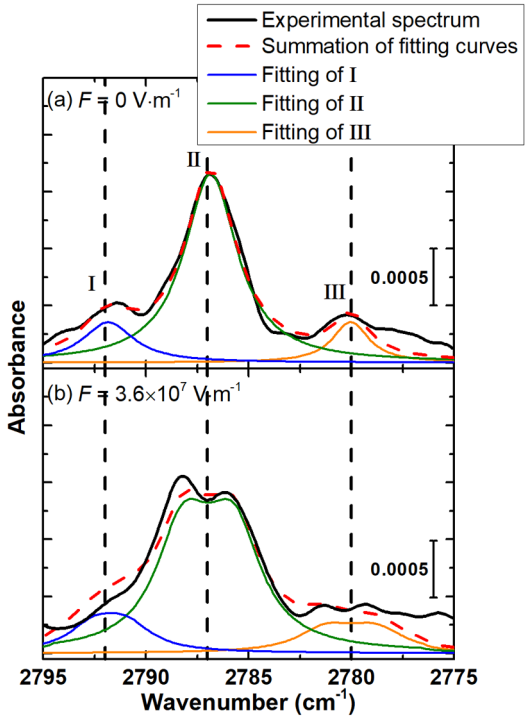

Figure 6. Experimental spectra (black-solid trace) of the HCl trimer band (II at 2787 cm^{-1}, labeled as T in Figure 1) and unidentified HCl multimer bands (I at 2792 cm^{-1} and III at 2780 cm^{-1}). The simulated spectra are shown by the red-dashed trace. (a) Spectrum at zero field. The spectrum was simulated by three Lorentzian curves in blue (I), green (II), and orange (III) color. (b) Spectrum at 3.6×10^7 V·m^{-1}. The spectrum was simulated by considering vibrational Stark broadening of the three bands. The vertical dashed lines indicate the center of the three bands. The Ar:HCl molar ratio in the sample was 390:1.

https://dx.doi.org/10.1021/acs.jpcb.0c02652
J. Phys. Chem. B 2020, 124, 4581–4589

trimer of the major isotopomer, $(H^{35}Cl)_3$. The corresponding vibrations of other isotopomers are expected to appear nearby: $(H^{35}Cl)_2H^{37}Cl$ at 2787 cm^{-1}, $(H^{35}Cl)_2H^{37}Cl$ at 2785.5 cm^{-1}, and $H^{35}Cl(H^{37}Cl)_2$ at 2784.5 cm^{-1}, as inferred from their gas-phase spectra.[13] These minor isotopomeric bands are not well resolved from the $(H^{35}Cl)_3$ band in the present spectral resolution and only contribute to broaden the spectral width of the major band. In addition, two neighboring bands appear at farther positions, 2792 and 2780 cm^{-1} (labeled as I and III, respectively), which probably originate from higher HCl multimers, as inferred from their reported frequencies.[2] Other vibrational modes than the asymmetric stretching mode of the cyclic HCl trimer appear in the low-frequency (<1000 cm^{-1}) region or have too weak oscillator strength to be observed, according to theoretical calculations.[13]

The Stark effect spectrum of the HCl trimer band measured at the field strength of 3.6×10^7 $V{\cdot}m^{-1}$ (Figure 6b) showed broadening of the bandwidth with a dip at its center. When the applied electric field was further increased, the band split into two components, as shown in Figure 1. These spectral changes are characteristic of the VSE of isotropically oriented oscillators that are observed when the external dc electric field is collinear with the p-polarization direction of the IR beam.[26,36,37] We analyzed the spectrum using a numerical simulation method. The spectrum at a moderate field strength (3.6×10^7 $V{\cdot}m^{-1}$) was chosen for this simulation to avoid the overlap between the trimer band (II) and other multimer bands (I and III), which would occur when the Stark broadening was too large in a strong field. The simulation procedure has been described in detail in previous studies.[36] In brief, the absorbance of a band is the sum of the absorbances (A) of the individual oscillators. The individual oscillators experience a Stark frequency shift, which depends on the angle between $\Delta\mu$ and F. Each of the three vibrational bands in Figure 6a at zero-field strength is fitted by a Lorentzian curve. The individual Lorentzian curves are then red- and blue-shifted according to eq 2, and these individual peaks are integrated to form a Stark effect spectrum. By comparing the experimental spectrum with the simulated one, with the Stark sensitivity factor ($\Delta\mu$) as the adjustable parameter, $\Delta\mu$ is estimated. The Stark sensitivity factor for the HCl trimer band was estimated to be $\Delta\mu_T = 4.5 \pm 0.5$ $cm^{-1}/(10^8$ $V{\cdot}m^{-1})$ in the field strength range of 3.6×10^7–3.0×10^8 $V{\cdot}m^{-1}$. Not surprisingly, this value was close to the Stark sensitivity factor estimated for the proton-donating HCl subunit of the HCl dimer: $\Delta\mu_{D2} = 5.1 \pm 0.5$ $cm^{-1}/(10^8$ $V{\cdot}m^{-1})$.

For simplicity, the spectral simulation was performed by assuming that the three (I, II, and III) bands had the same $\Delta\mu$ value because the intensities of bands I and III were too weak to estimate their $\Delta\mu$ values through spectral fitting of the individual bands. This approximation did not significantly affect the simulation results at low field strengths such as one shown in Figure 6b, where the overlap between these bands was insignificant. Furthermore, we neglected the absorbances of minor isotopomers in the trimer band (II). The minor isotopomer bands introduce an asymmetric feature in the low-frequency region of the Stark effect spectrum because their frequencies are lower than that of the $(H^{35}Cl)_3$ band. This effect was almost invisible in the spectrum of Figure 6b and buried in the large Stark broadening of the $(H^{35}Cl)_3$ band. The asymmetric profile was more discernible in the Stark effect difference spectrum measured in weak (10^6 $V{\cdot}m^{-1}$) electric fields (Figure S3 in the Supporting Information).

The observation that the trimer band shows only a reversible spectral broadening without a shift in position indicates the stability of the cyclic trimer structure under the applied electric field. This result was supported by the observation that the integrated absorbance of the band did not change with the increase in electric field strength (Figure S4 in the Supporting Information). It showed that the applied electric field neither reorients the transition dipole moment of the trimer because of its zero permanent dipole moment[2,6] nor breaks the cyclic trimer structure. The stable HCl trimer structure was also consistent with the observation that new dimer peaks did not appear as the electric field was increased (Figure 1). If the ring structure of the trimer was opened by the applied electric field, then D1-like features would appear in the spectra.

4. SUMMARY AND CONCLUSIONS

The application of a dc electric field of strength up to 4×10^8 $V{\cdot}m^{-1}$ to the HCl dimers and trimers isolated in the Ar matrix revealed interesting spectroscopic and dynamic behaviors of these complexes in an electric field. The RAIR spectra showed that the H−Cl stretching vibrations of the proton-acceptor and -donor subunits of the HCl dimer exhibited a red frequency shift that was linearly proportional to the electric field strength above $\sim 1 \times 10^8$ $V{\cdot}m^{-1}$. This indicated that the HCl subunits of the dimer were reoriented along the direction of the applied electric field. The reorientation mechanism was investigated by observing the Stark response of HCl−DCl and DCl−HCl structural isomers. While the ν_{donor}^{HCl} intensities of these heterodimers increased with an increase in the electric field strength, the ν_{donor}^{DCl} intensities decreased. This trend revealed tunneling inversion of HCl (or DCl) by an electric field as the reorientation mechanism, which interconverted the proton-acceptor and -donor subunits in the dimer. The interconversion of dimers occurred reversibly with the applied field strength. The yield of dimer interconversion as a function of the field strength was explained by a thermodynamic model that accounted for the enthalpy and entropy changes associated with the inversion of the HCl subunits in an electric field.

The applied electric field increased the absorbance of the H−Cl vibration of the proton-acceptor subunit of dimers continually and extraordinarily beyond the absorbance limit expected for field-oriented chromophores. This phenomenon may be explained by an increase in the vibrational transition dipole moment under the influence of a strong electric field.

The asymmetric stretching band of the HCl trimers exhibited only Stark broadening, which indicated the stability of a cyclic trimer structure in the electric field. Analysis of the VSE spectra of the HCl dimers and trimers yielded the Stark sensitivity factors of the corresponding bands as $\Delta\mu_{D1} = 2.3 \pm 0.2$ $cm^{-1}/(10^8$ $V{\cdot}m^{-1})$, $\Delta\mu_{D2} = 5.1 \pm 0.5$ $cm^{-1}/(10^8$ $V{\cdot}m^{-1})$, and $\Delta\mu_T = 4.5 \pm 0.5$ $cm^{-1}/(10^8$ $V{\cdot}m^{-1})$, without the correction for local fields.

These observations of the matrix-isolated HCl dimers and trimers can help us understand the response of hydrogen-bonded molecular complexes to the intermolecular electric fields present in condensed-phase environments, which have strengths on the order of 10^8 $V{\cdot}m^{-1}$. It is anticipated that hydrogen-bonded complexes with an open-chain structure may undergo rapid tunneling interconversion and rearrangement by electric fields from neighboring molecules, while those with a closed cyclic structure may be relatively more stable.

https://dx.doi.org/10.1021/acs.jpcb.0c02652
J. Phys. Chem. B 2020, 124, 4581−4589

■ ASSOCIATED CONTENT

Supporting Information

The Supporting Information is available free of charge at https://pubs.acs.org/doi/10.1021/acs.jpcb.0c02652.

(1) A plot of frequency shifts of the HCl monomer and dimer bands, (2) thermodynamic model for dimer interconversion, (3) difference absorbance spectra of the HCl trimer band, and (4) constant absorbance of the trimer band in an electric field (PDF)

■ AUTHOR INFORMATION

Corresponding Author

Heon Kang − *Department of Chemistry, Seoul National University, Seoul 08826, Republic of Korea;* orcid.org/0000-0002-7530-4100; Phone: +82 2 875 7471; Email: surfion@snu.ac.kr; Fax: +82 2 889 8156

Authors

Hani Kang − *Department of Chemistry, Seoul National University, Seoul 08826, Republic of Korea*

Youngwook Park − *Department of Chemistry, Seoul National University, Seoul 08826, Republic of Korea*

Sunghwan Shin − *Department of Chemistry, Seoul National University, Seoul 08826, Republic of Korea*

Complete contact information is available at: https://pubs.acs.org/10.1021/acs.jpcb.0c02652

Notes

The authors declare no competing financial interest.

■ ACKNOWLEDGMENTS

This work was supported by the Samsung Science and Technology Foundation (SSTF-BA1301-04).

■ REFERENCES

(1) Kang, H.; Park, Y.; Kim, Z. H.; Kang, H. Electric Field Effect on Condensed-Phase Molecular Systems. VI. Field-Driven Orientation of Hydrogen Chloride in an Argon Matrix. *J. Phys. Chem. A* **2018**, *122*, 2871−2876.

(2) Maillard, D.; Schriver, A.; Perchard, J. P.; Girardet, C. Study of Hydracids Trapped in Monatomic Matrices. I. Near Infrared Spectra and Aggregate Structures. *J. Chem. Phys.* **1979**, *71*, 505−516.

(3) Katz, B.; Ron, A.; Schnepp, O. Far-Infrared Spectrum of HCl Dimers. *J. Chem. Phys.* **1967**, *47*, 5303−5306.

(4) Barnes, A. J.; Hallam, H. E.; Scrimshaw, G. F. Infra-Red Cryogenic Studies. Part 1.—Hydrogen Halide Multimers. *Trans. Faraday Soc.* **1969**, *65*, 3150−3158.

(5) Girardet, C.; Robert, D. Interpretation of the Far Infrared Spectra of the Dimers of HCl and of DCl Trapped in Monoatomic Solids. *J. Chem. Phys.* **1973**, *58*, 4110−4130.

(6) Hallam, H. E. *Vibrational Spectroscopy of Trapped Species: Infrared and Raman Studies of Matrix-Isolated Molecules, Radicals and Ions*; University Microfilms International: Ann Arbor, MI, 1996.

(7) Ortlieb, M.; Birer, Ö.; Letzner, M.; Schwaab, G. W.; Havenith, M. Observation of Rovibrational Transitions of HCl,$(HCl)_2$, and H_2O-HCl in Liquid Helium Nanodroplets. *J. Phys. Chem. A* **2007**, *111*, 12192−12199.

(8) Ohashi, N.; Pine, A. S. High Resolution Spectrum of the HCl Dimer. *J. Chem. Phys.* **1984**, *81*, 73−84.

(9) Pine, A. S.; Howard, B. J. Hydrogen Bond Energies of the HF and HCl Dimers from Absolute Infrared Intensities. *J. Chem. Phys.* **1986**, *84*, 590−596.

(10) Schuder, M. D.; Lovejoy, C. M.; Lascola, R.; Nesbitt, D. J. High Resolution, Jet-Cooled Infrared Spectroscopy of $(HCl)_2$: Analysis of ν_1 and ν_2 HCl Stretching Fundamentals, Interconversion Tunneling, and Mode-Specific Predissociation Lifetimes. *J. Chem. Phys.* **1993**, *99*, 4346−4362.

(11) Imura, K.; Kasai, T.; Ohoyama, H.; Naaman, R. Focusing of DCl and HCl Dimers by an Electrostatic Hexapole Field: The Role of the Tunneling Motion. *J. Chem. Phys.* **1999**, *110*, 355−358.

(12) Latajka, Z.; Scheiner, S. Structure, Energetics and Vibrational Spectra of H-Bonded Systems. Dimers and Trimers of HF and HCl. *Chem. Phys.* **1988**, *122*, 413−430.

(13) Fárník, M.; Nesbitt, D. J. Intramolecular Energy Transfer between Oriented Chromophores: High-Resolution Infrared Spectroscopy of HCl Trimer. *J. Chem. Phys.* **2004**, *121*, 12386−12395.

(14) Skvortsov, D.; Choi, M. Y.; Vilesov, A. F. Study of HCl Clusters in Helium Nanodroplets: Experiments and ab Initio Calculations as Stepping Stones from Gas Phase to Bulk. *J. Phys. Chem. A* **2007**, *111*, 12711−12716.

(15) Han, J.; Wang, Z.; McIntosh, A. L.; Lucchese, R. R.; Bevan, J. W. Investigation of the Ground Vibrational State Structure of $H^{35}Cl$ Trimer Based on the Resolved *K J* Substructure of the ν_5 Vibrational Band. *J. Chem. Phys.* **1994**, *100*, 7101−7108.

(16) Bemish, R. J.; Chan, M. C.; Miller, R. E. Molecular Control Using DC Electric Fields: Quenching of the Tunneling in HF Dimer. *Chem. Phys. Lett.* **1996**, *251*, 182−188.

(17) Fritz, J. J.; Fuget, C. R. Vapor Pressure of Aqueous Hydrogen Chloride Solutions, 0° to 50°C. *Chem. Eng. Data Ser.* **1956**, *1*, 10−12.

(18) Kim, Y.-K.; Rudd, M. E. Binary-Encounter-Dipole Model for Electron-Impact Ionization. *Phys. Rev. A: At., Mol., Opt. Phys.* **1994**, *50*, 3954−3967.

(19) Wetzel, R. C.; Baiocchi, F. A.; Hayes, T. R.; Freund, R. S. Absolute Cross Sections for Electron-Impact Ionization of the Rare-Gas Atoms by the Fast-Neutral-Beam Method. *Phys. Rev. A: At., Mol., Opt. Phys.* **1987**, *35*, 559−577.

(20) Hodgson, A.; Haq, S. Water Adsorption and the Wetting of Metal Surfaces. *Surf. Sci. Rep.* **2009**, *64*, 381−451.

(21) Brown, D. E.; George, S. M.; Huang, C.; Wong, E. K. L.; Rider, K. B.; Smith, R. S.; Kay, B. D. H_2O Condensation Coefficient and Refractive Index for Vapor-Deposited Ice from Molecular Beam and Optical Interference Measurements. *J. Phys. Chem.* **1996**, *100*, 4988−4995.

(22) Schulze, W.; Kolb, D. M. Density and Refractive Index of Solid Layers of Noble Gases and Sulphur Hexafluoride. *J. Chem. Soc., Faraday Trans. 2* **1974**, *70*, 1098−1105.

(23) Shin, S.; Kim, Y.; Moon, E.-S.; Lee, D. H.; Kang, H.; Kang, H. Generation of Strong Electric Fields in an Ice Film Capacitor. *J. Chem. Phys.* **2013**, *139*, 074201.

(24) Bacalis, N. C.; Papaconstantopoulos, D. A.; Pickett, W. E. Systematic Calculations of the Band Structures of the Rare-Gas Crystals Neon, Argon, Krypton, and Xenon. *Phys. Rev. B: Condens. Matter Mater. Phys.* **1988**, *38*, 6218−6226.

(25) Tsekouras, A. A.; Iedema, M. J.; Cowin, J. P. Amorphous Water-Ice Relaxations Measured with Soft-Landed Ions. *Phys. Rev. Lett.* **1998**, *80*, 5798−5801.

(26) Andrews, S. S.; Boxer, S. G. Vibrational Stark Effects of Nitriles I. Methods and Experimental Results. *J. Phys. Chem. A* **2000**, *104*, 11853−11863.

(27) Bublitz, G. U.; Boxer, S. G. Stark Spectroscopy: Applications in Chemistry, Biology, and Materials Science. *Annu. Rev. Phys. Chem.* **1997**, *48*, 213−242.

(28) Fried, S. D.; Boxer, S. G. Measuring Electric Fields and Noncovalent Interactions Using the Vibrational Stark Effect. *Acc. Chem. Res.* **2015**, *48*, 998−1006.

(29) Park, Y.; Kang, H.; Kang, H. Brute Force Orientation of Matrix-Isolated Molecules: Reversible Reorientation of Formaldehyde in an Argon Matrix toward Perfect Alignment. *Angew. Chem., Int. Ed.* **2017**, *56*, 1046−1049.

(30) Perchard, J. P.; Maillard, D.; Schriver, A.; Girardet, C. Structures of HCl and HBr Polymers in Nitrogen Matrix Derived from Infrared and Raman Data: Comparison with Argon Matrix. *J. Raman Spectrosc.* **1981**, *11*, 406−415.

(31) Hush, N. S.; Reimers, J. R. Vibrational Stark Spectroscopy. 1. Basic Theory and Application to the CO Stretch. *J. Phys. Chem.* **1995**, *99*, 15798−15805.
(32) Bottcher, C. J. F. *Theory of Electric Polarization*, 2nd ed.; Elsevier: Amsterdam, 1973.
(33) Kang, H.; Maurais, J.; Park, Y.; Ayotte, P.; Kang, H. Electric Field Effect on Condensed-Phase Molecular Systems. VIII. Vibrational Stark Effect and Dipolar Inversion in Carbon Monoxide Crystal. *J. Phys. Chem. C* **2019**, *123*, 31262−31271.
(34) Dean, J. A.; Lange, N. A. *Lange's Handbook of Chemistry*; McGraw-Hill: New York, 1973.
(35) Burrus, C. A. Stark Effect at 0.93, 1.18, and 1.5 Millimeters Wavelength: DCl, DBr, and DI. *J. Chem. Phys.* **1959**, *31*, 1270−1272.
(36) Shin, S.; Kang, H.; Cho, D.; Lee, J. Y.; Kang, H. Effect of Electric Field on Condensed-Phase Molecular Systems. II. Stark Effect on the Hydroxyl Stretch Vibration of Ice. *J. Phys. Chem. C* **2015**, *119*, 15596−15603.
(37) Kang, H.; Shin, S.; Park, Y.; Kang, H. Electric Field Effect on Condensed-Phase Molecular Systems. III. The Origin of the Field-Induced Change in the Vibrational Frequency of Adsorbed CO on Pt (111). *J. Phys. Chem. C* **2016**, *120*, 17579−17587.

https://dx.doi.org/10.1021/acs.jpcb.0c02652
J. Phys. Chem. B 2020, 124, 4581−4589